Modelling of Material Damage of CFC and W Macro-Brush Divertor Targets under ELMs and Disruptions in Plasma Gun Facilities and Prediction for ITER

B. Bazylev 1), G. Janeschitz 2), I. Landman 1), S. Pestchanyi 1), A. Loarte 3), G. Federici 4), M. Merola 4), J. Linke 5), J. Compan 5), T. Hirai 5), O. Ogorodnikova 6), A Zhitlukhin 7), V. Podkovyrov 7), N. Klimov 7), V. Safronov 7), I. Garkusha 8)

1)Forschungszentrum Karlsruhe, IHM, P.O. Box 3640, 76021 Karlsruhe, Germany
2)Forschungszentrum Karlsruhe, Fusion, P.O. Box 3640, 76021 Karlsruhe, Germany
3)EFDA Close Support Unit Garching, Boltmannstr.2, D-85748 Garching bei München, Germany
4)ITER International Team, Garching Working Site, Boltmannstr.2, D-85748 Garching bei München, Germany
5)Association Euratom- Institut für Plasmaphysik Jülich, D-5245 Jülich, Germany
6)Département de Recherches sur la Fusion Contrôlée, Association Euratom-CEA, CEA-Cadarache F-13108, Saint Paul Lez Durance Cedex, France
7)SRC RF TRINITI, Troitsk, 142190, Moscow Region, Russia
8)Institute of Plasma Physics of the National Science Centre, Kharkov Institute of Physics and Technology, 61108 Kharkov, Ukraine

E-mail of main author: bazylev@ihm.fzk.de

Abstract. Operation of ITER at high fusion gain is assumed to be the H-mode. A characteristic feature of this regime is the transient release of energy from the confined plasma onto plasma facing components (PFCs) by multiple, which can play a determining role in the erosion rate and lifetime of these components. During the intense transient events in ITER the evaporation (CFC, W) and surface melting, melt motion, and melt splashing (W) are seen as the main mechanisms of PFC erosion. The expected erosion of the ITER plasma facing components under transient energy loads can be properly estimated by numerical simulations validated against target erosion of the experiments at the plasma gun facilities QSPA-T, MK-200UG and QSPA-Kh50. Within the collaboration established between EU fusion programme and the Russian Federation, PFC components manufactured according to the EU specifications for the ITER divertor targets, have been exposed to ITER ELM-like and disruption-like loads in plasma gun facilities at TRINITI. The measured material erosion data have been used to validate the codes, PEGASUS, MEMOS, PHERMOBRID and FOREV-2, which are then applied to model the erosion of the divertor and main chamber ITER PFCs under the expected loads in ITER. Numerical simulations performed for the expected ITER-like loads demonstrated: a significant erosion of the CFC target is expected for ITER-like loads in excess of ~ 0.5 MJ/m^2, caused by the inhomogeneous structure of the material; the W macrobrush structure is effective in preventing gross melt layer displacement during ELM-like loads leading to the overall erosion of W in these conditions being determined by the evaporation of the material. Optimization of macrobrush geometry in order to minimize erosion under ITER-like transient loads has been carried out. The erosion of the dome armour and the gaps between the divertor cassettes under the radiation from the plasma shield is numerically investigated for ITER disruption conditions. Different mechanisms of melt splashing are analyzed and implemented in the code MEMOS. For estimation of the W crack formation an analytical model that links the crack depth with the characteristic size of the crack mesh is proposed.

1. Introduction

Operation of ITER in high fusion gain regimes is assumed to be in H-mode [1]. A characteristic feature of this regime is the transient release of energy from the confined plasma onto plasma facing components (PFCs) by multiple ELMs, which may mainly determine the erosion rate and lifetime of these components [2]. During one ITER discharge about 10^3 ELMs are expected. Similarly, the transient power fluxes to which PFCs are subject during disruptions can affect significantly their lifetime [3] and during ITER operation several hundred disruptions, interspaced by ELMs may occur. During disruptions and ELMs energy released is deposited onto the main wall and divertor. The expected fluxes on the ITER plasma facing components during transients are [4]: I) Divertor target. Type I ELM energy fluxes : 0.5 – 4 MJ/m^2 in timescales of 300-600 μs. Thermal quench energy fluxes of 2 - 13 MJ/m^2 in timescales of 1-3 ms. II) Main wall. Type I ELM energy fluxes: 0.5 – 2 MJ/m^2 in timescales of 300-600 μs. Thermal quench energy fluxes of 0.5 - 5 MJ/m^2 in timescales of 1-3 ms. Mitigated disruption radiative loads of 0.1 – 2 MJ/m^2 in timescales of 0.2- 1.0 ms.

CFC and tungsten macrobrush armour are foreseen as PFC for ITER divertor and dome. During intense transient events in ITER as the disruptions and ELMs evaporation (CFC, W) and surface melting (W) are seen as the main mechanisms of PFC erosion. Melt motion in a thin layer of tungsten may produce surface roughness and droplet splashing thus causing erosion of the target. Numerical simulations [5] demonstrated that the macrobrush geometry prevents violent melt motion and decreases total damage of the target surface. Numerical simulations aiming optimization of the W macrobrush structure to decrease the total erosion was carried out [6]. Due to rather different heat conductivities of CFC fibers a noticeable erosion of the PAN fibers may occur at a rather small heat loads at which the damage to the tungsten armour is not substantial. Crack formation inside the CFC armour can lead to a significant drop of the heat conductivity, which intensifies the erosion and brittle destruction (BD) of the CFC armour may occur. A rather intense crack formation was observed also for the W targets under moderate plasma heat loads observed at the QSPA facility [7-9].

The expected erosion of the ITER plasma facing components under transient energy loads can be really estimated by numerical simulation using codes validated against target erosion obtained in the experiments at the plasma gun facilities QSPA-T, MK-200UG and QSPA-Kh50 that present a natural choice for the generation of required load. The impact mechanism of pulsed power of the plasma stream propagating along the inclined magnetic field on the aperture of several cm comes most close to the ITER off-normal conditions.

Within collaboration established between EU fusion programme and the TRINITI and Kurchatov Institutes in the Russian Federation, components manufactured according the EU specifications for the ITER divertor targets, have been exposed to ITER ELM-like and disruption-like loads in plasma gun facilities at TRINITI [8]. The measured material erosion has been used to validate the modelling codes, PEGASUS, MEMOS, PHERMOBRID and FOREV-2, which are then applied to model the erosion of the divertor and main chamber ITER PFCs under the expected loads in ITER. The main results of the experiments and numerical simulations are described in Section 2. Other devices such as the tokamak TEXTOR, the electron beam test facility JUDITH and pulsed Nd:YAG laser are also used for the verification of the codes MEMOS, PHERMOBRID. The calculated dependences of the crater depth vs. heat loads are in good agreement with the dependences obtained in the in the e-beam and laser experiments.

In frame of the material damage simulations the code FOREV-2 [10] is applied for calculation of parameters of the plasma shield being formed from evaporated material in front of the target, which are further used in the codes MEMOS and PHERMOBRID. In case of metallic target, the surface melting and vaporisation is simulated and their roles compared using the code MEMOS that describes two-dimensional surface processes. The melt motion in MEMOS is described taking into account the surface tension, viscosity of molten metal, and the radiative losses from the hot tungsten surface. The plasma pressure variations along the divertor plate, as well as the gradient of surface tension and the Lorentz force of the currents crossing the melt layer immersed in strong magnetic field, produce the melt acceleration. The melt splashing generated by growth of surface waves due to the “evaporation” instability and due to the Kelvin-Helmholtz instability are implemented into the code. The influence of Lorenz force on melt motion is validated by the experiments in QSPA-Kh50 facility [11] Numerical simulation results are in a rather good agreement with the measured melt layer displacement caused by the Lorenz force. First estimation of the melt splashing due to the Kelvin-Helmholtz was done and demonstrated that the weak and moderate ITER ELMs does not cause significant droplet splashing.

The CFC armour erosion is calculated by the 3-dimensional code PHEMOBRID [12] in which 3D heat conductivity properties of CFC accounting degradation of the matrix due to the crack formation leading to the drop of it’s heat conductivity as well as phenomenological model of BD are implemented. The volumetric energy of impacting electrons is calculated using a Monte-Carlo code.

Numerical simulations performed for the expected ITER-like loads demonstrated that significant erosion of the CFC target is expected for ITER-like loads in excess of ~ 0.5 MJ/m^2, caused by the inhomogeneous structure of the material. On the other hand, the W macrobrush structure is effective in preventing gross melt layer displacement during ELM-like loads leading to the overall erosion of W in these conditions being determined by the evaporation of the material. Optimization of macrobrush geometry to minimize erosion under ITER-like transient loads is done [6].

For estimation of the W crack formation at the W surface an analytical model, linking the crack depth with the characteristic size of the crack mesh is proposed. The model takes into account the tensile thermostress in the resolidified layer and its relaxation due to the cracks. This model described in Section 3 is the first approximation for the real situation with tungsten cracking [13].

The heat load of a single giant ELM with energy density > 2.5 MJ/m^2 or a disruption causes a plasma shield being formed from evaporated material in front of the target. This shielding layer is a source of intense radiation at GW/m^2 level with durations of 0.5 ms for ELMs and up to 10 ms for the disruptions. Numerical simulations performed by code MEMOS for multiple disruptions with the energy deposition Q of 10-30 MJ/m^2 and the duration τ of 1-10 ms and of multiple ELMs with Q= 1-3 MJ/m^2 and τ= 0.1-0.5 ms demonstrate that intense radiation from the vapour shield may leads to enhanced erosion of nearby dome armour and gaps between divertor cassettes. Such effects should be taken into account in design of the dome and divertor cassettes. [6]

2. Simulation of the CFC and W macrobrush target erosion under multiple ELM-like plasma heat loads.

Experiment. The targets consisted of separate tungsten and CFC elements of sizes 9.5x9.5x3 mm^3 and 19.5x19.5x3 mm^3 brazed to a supporting stainless steel plate with 0.5 mm gaps between brushes was exposed to series of repeated plasma pulses (100 in each series) with energy density in a range of 0.5-1.5 MJ/m^2 and 0.5 ms duration. The target was placed on a heater, which provided target preheating up to 500ºC. The plasma stream has Gaussian profile with half width of 8 cm and was inclined under angle of 30º to the target surface. The plasma pressure varied in range of 0.3 – 0.9 MPa.

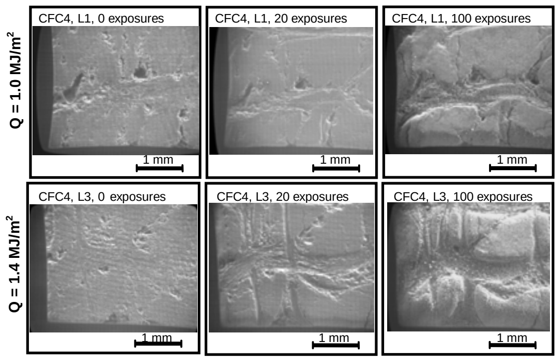

FIG. 2.. The view of the CFC tile surface obtained by means of electron microscope

CFC and tungsten targets after every series of 10-20 pulses, the target was cooled down and investigated: a) the target was weighted to determine mass loss, b) the surface was inspected using electron and optical microscopes to detect the presence of cracks and measure of PAN-fibre erosion in CFC. After a total of 100 pulses, the surface profile of each target was measured by laser profilometer to find the value of material losses during post-mortem characterisation in FZJ. According to electron microscope observation the erosion of CFC macrobrushes was determined mainly by erosion of PAN-fibres (See Fig. 1): at the energy density Q< 0.5 MJ/m^2 erosion was negligible; at 0.6<Q<0.9 MJ/m^2 the erosion of PAN-fibres was observed not only near the edges but also on the total surface of the tiles after 100 exposures; at 0.9<Q<1.3 MJ/m2 the noticeable erosion of PAN-fibres took place after 50 exposures; at 1.3<Q<1.4 MJ/m2 the significant erosion of PAN-fibres took place already after 10 exposures.

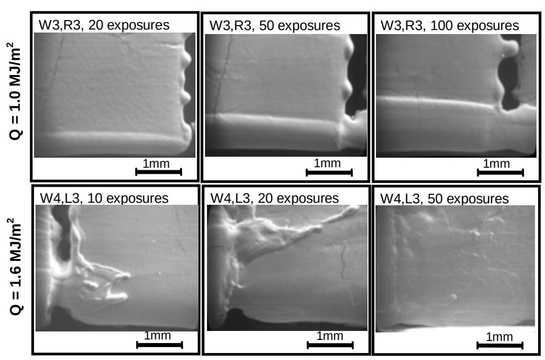

FIG. 3. The view of the tungsten tile surface obtained by means of electron microscope

According to this characterisation the erosion of tungsten macrobrushes was determined mainly by melt layer movement and droplets ejection (See Fig. 2): at the energy density Q<0.4 MJ/m^2 erosion was negligible; at 0.4<Q<1.0 MJ/m^2 took place melting of the plasma facing edges of the tiles; at 1.0<Q<1.3 MJ/m^2 melting was observed not only near the edges but also on the total surface of the tiles but droplet ejection did not took place; as a the results of melt layer movement along the plasma stream direction and accumulation on the plasma shadow edges separate bridges between tiles was formed after 50 exposures; at 1.3<Q<1.6 MJ/m^2 - bridges was formed already after 10 exposures; as a result of this process gaps between tiles was covered by remelted tungsten after 50 exposures; droplet ejection was observed at Q> 1.3 MJ/m^2. 1.6 MJ/m^2. The appropriated average erosion of the sample was equalled to 0.06 µm/shot for the energy load Q= 1.6 MJ/m^2. Cracks formation was observed at the energy density Q>0.8 MJ/m^2 In the energy density range from 0.8 MJ/m^2 to 1.0 MJ/m^2 the two types of cracks formed the grids on the surface. The post-mortem metallography show that the depth of the cracks type 1 and type 2 equal to about 500 µm and 50 µm, respectively. At the energy density more 1.0 MJ/m2 the cracks formed grid with the characteristic cell size 50 µm and are remelted in each pulses.

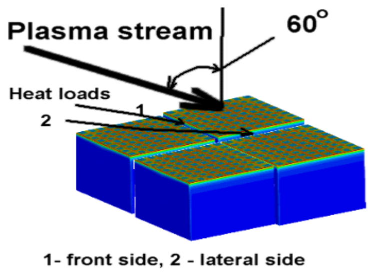

FIG. 3. Sketch of target geometry used in numerical simulations.

Numerical simulations. The sketch of the target geometry used in the 3D calculations is shown in Fig.3: sizes of brushes and gaps are the same as in experiments. The following model structure of CFC brush was assumed: pitch bundles (diameter d=0.06 cm) are in the vertical direction and PAN-bundles (d=0.06 cm) are in both horizontal directions. The graphite matrix fills the space between the bundles. The regular brush structure (pitch bundles) can be seen in Fig. 3 (and in Fig. 4). Heat conductivity coefficients for all these CFC elements are different and are fitted by the well-known expression: $\lambda \approx A + B/T + C/T^2$. For each CFC element coefficients A,B,C are fitted so that: at T=400K $\lambda_{pitch} = 2.7$ W/cmK, $\lambda_{PAN} = 1.2$ W/cmK; and at T=3500 K $\lambda_{pitch} = 0.45$ W/cmK, $\lambda_{PAN} = 0.13$ W/cmK ($\lambda_{PAN} = \lambda_{matrix}$).

The numerical simulations were carried out for the target preheated up to 500°C. The absorbed energy density Q was varied in a range 0.5-1.5 MJ/m^2 with the pulse duration of τ =0.5 ms, the plasma pressure at the inclined target of 0 and 0.2 MPa was assumed. To clarify depends of CFC erosion on ELM duration simulations for Q= 1 MJ/m^2 with pulse duration τ varying in the range 0.25 - 0.6 ms were done.

Due to rather low heat conductivity noticeable evaporation of the PAN bundles occur at the heat loads Q> 0.7 MJ/m^2 and plasma shielding by evaporated atoms decreases heat flux at the target surface. For accounting shielding effect the following simple model is implemented: heat flux at the target surface is calculated in accordance with the following equation $W(t) = W_0 \exp(-h(t)/h_0)$, where W_0 - incident heat flux, h_0 = 1.5 μm - vapour shield thickness, and $h(t)$ - thickness of evaporated material. The heating of the frontal and lateral sides of brushes are determined by the inclination angle and the gap width and calculated in accordance with the expressions derived in Ref. [6] for brush geometry. The melt motion along W brushes is simulated by the code MEMOS in accordance with [6].

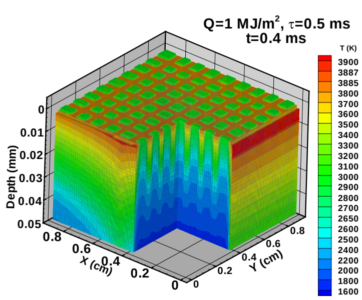

FIG. 3. Calculated temperature distribution inside CFC brush

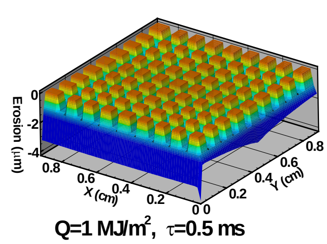

FIG. 4. Final calculated erosion profile of CFC brush

CFC targets. Numerical simulations demonstrated that due to high heat conductivity pitch bundles sink mainly energy deposited at the target surface. Dependence of the absorbed energy versus incident energy calculated for the pitch bundles well agrees with measured one by CFC calorimeter. Typical temperature distribution inside CFC brushes is shown in Fig. 3 for the reference scenario Q=1 MJ/m^2. For example at t=0.4 ms due to large difference in the heat conductivities surface temperature of PAN bundles reaches approximately 3800 K whereas pitch bundles remains rather cold T=3000K. The frontal and lateral brush edges are significantly overheated also. That leads to the negligible erosion of pitch bundles and intense evaporation erosion of the PAN ones and lateral and frontal edges (Fig. 4). Calculated dependences of PAN and pitch bundles erosion as functions of absorbed energy are shown in Fig. 5. Good agreement with measured PAN bundle erosion achieved if shielding was taken into account. Dependence of CFC erosion on pulse duration (Fig. 6) demonstrates that short ELMs are more dangerous.

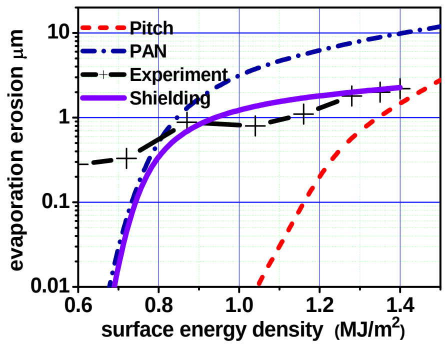

FIG. 5. Calculated and measured PAN bundles erosion vs. of absorbed energy

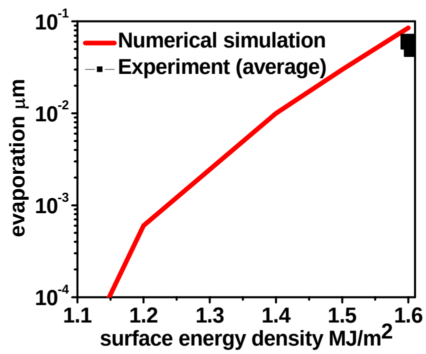

FIG. 7. Calculated erosion of W brush due to evaporation vs. absorbed energy

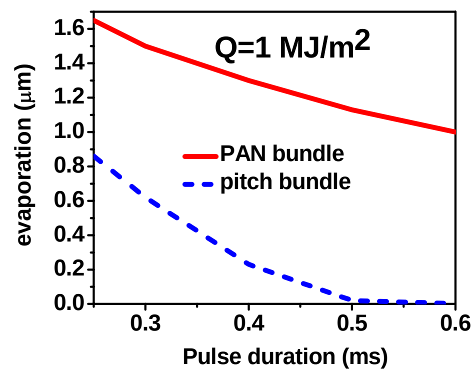

FIG. 6. Calculated erosion of PAN and pitch bundles vs. pulse duration. Q=1 MJ/m^2

3D numerical simulations carried out for **W macrobrush target** demonstrated that melting of the frontal and lateral brush edges starts at Q>0.7 MJ/m^2. Calculated dependences W brush evaporation as functions of absorbed energy (shown in Fig. 7) demonstrated rather good agreement with measured and shows that evaporation mainly responsible for the W mass losses for heat load Q<1.6 MJ/m^2.

3. Simulation of cracks in tungsten under ITER specific heat loads

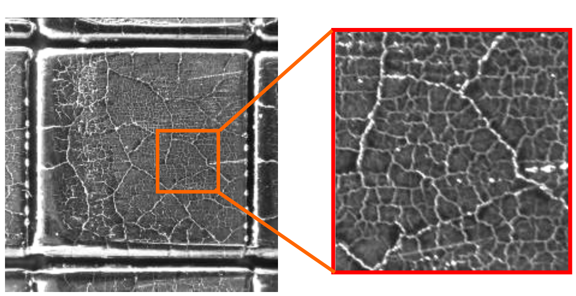

FIG. 8. Tungsten tile surface after 100 plasma shots in QSPA facility irradiated with heat load of 0.9 MJ/m^2 during 0.5 ms.

The experiments in the QSPA facility carried out shown an intense tungsten surface cracking under the ITER ELM conditions at the divertor (Fig. 8). Analysis of the thermophysical parameters of tungsten revealed its large potential for cracking: the thermostress due to thermal expansion from room temperature to the melting temperature is more than one order of the magnitude larger than the tensile strength of tungsten. The cracks at the tungsten surface arise due to the thermostress, developed in the sample under severe heat loads characteristic for ITER ELMs and disruptions. The thermostress generated in the tungsten sample under the heated surface due to two different reasons. The first one is the temperature gradient, which produces compressive stress at the surface. The second one is the tensile stress generated during cool-down of the resolidified layer if the surface has been melted. The second mechanism of crack generation was investigated, because the tensile stress seems more critical for development of cracks.

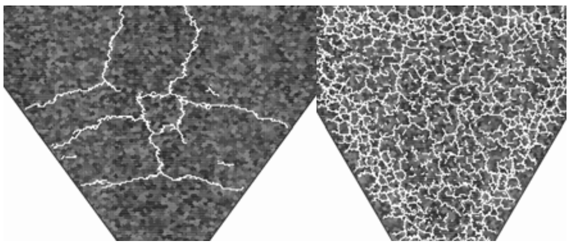

FIG. 9. Result of the PEGASUS-3D simulation of the cracks developed in tungsten sample after irradiation with heat load of 0.9 MJ/m^2 and 0.5 ms time duration.

An analytical model for cracks formation in tungsten under the tensile stress in the resolidified layer has been proposed. The model predicts the development of cracks of several characteristic scales. The primary crack pattern, a rough mesh of cracks is developed during cooling of the sample to some intermediate temperature, higher than the final sample temperature. The primary cracks relax the thermostress inside the primary meshes, so the secondary cracks inside the primary meshes should have smaller depth then the primary ones and so on. An analytical model explains the existence of the secondary fine grain crack network by the thermostress relaxation due to the primary cracks in the resolidified layer.

The thermo-mechanical code PEGASUS-3D has been developed for numerical simulation of tungsten surface cracking under the action of the thermostress arising in thin resolidified surface layer. Numerical simulation of the experiments with the melting of a thin surface layer of tungsten resulted in qualitative agreement between the crack patterns obtained in the experiments with the pattern seen in the simulations (See Fig. 9 where Primary cracks on depth of 200 μm are shown in the left hand panel. Right hand panel illustrates both primary and secondary crack pattern at the sample surface.). Both, experimentally observed and simulated crack networks consist of a coarse primary meshes formed of deep cracks and each coarse mesh is covered by shallower secondary crack grid with one order of the magnitude smaller depth.

4. Conclusion.

Within the collaboration established between EU fusion programme and the Russian Federation, PFC components manufactured according to the EU specifications for the ITER divertor targets, have been exposed to ITER ELM-like and disruption-like loads in plasma gun facilities at TRINITI. Under ITER ELM-like plasma heat loads the CFC erosion was mainly determined by PAN-fiber evaporation. Erosion was negligible at the energy density less than 0.5 MJ/m^2. The noticeable erosion of CFC was observed at the energy 1.5 MJ/m^2 and average mean of it was 0.3 μm per shot. The value of PAN-fibre erosion was less than 2.5 μm per shot over all investigated energy density range.

The tungsten erosion was mainly due to melt layer movement and droplets ejection. Erosion was negligible at the energy density less than 0.5 MJ/m^2. The noticeable erosion of tungsten was observed at the energy 1.5 MJ/m^2 and average mean of it was 0.06 μm per shot. At this energy the gaps filling by melt layer were observed. It is expected that in ITER this effect will be absence because the plasma pressure will be a factor of ~ 10 lower of compare with this experiment.

The measured material erosion data have been used to validate the codes, PEGASUS, MEMOS, PHERMOBRID and FOREV-2, which are then applied to model the erosion of the divertor and main chamber ITER PFCs under the expected loads in ITER. The numerical simulations of CFC damage under the QSPA conditions are in good qualitative and quantitative agreements with the experiments. A significant erosion of brush edges and PAN bundles at Q>0.7 MJ/m^2 and pitch bundle erosion at Q>1.3 MJ/m^2 were obtained. The numerical simulations of W-target heating under QSPA conditions demonstrated melting of the brush edges at Q>0.7 MJ/m^2 and brush surface melting for Q>1 MJ/m^2. The calculated evaporation erosion is in a good agreement with the measured one.

The numerical simulations demonstrated that an optimal inclination angle of brush surface can be found for each given inclination angle of the plasma stream and the other parameters of macrobrush elements. Numerical simulations demonstrated that in case of disruptions a significant erosion of dome armour can be expected.

Acknowledgement

This work, supported by the European Communities under the Contract EFDA/05-1305 of Association between EURATOM and Forschungszentrum Karlsruhe, was carried out within the framework of the European Fusion Development Agreement. The views and options expressed herein do not necessarily reflect those of the European Commission.

References

[1] ITER Physics Basis, Nucl. Fusion **39** (1999) 2137,
[2] FEDERICI, G., et al, “Key ITER plasma edge and plasma–material interaction issues”, J. Nucl. Mat., **313-316** (2003), 11-22
[3] LOARTE, A., et al., Proc. 20th IAEA Conference, Vilamoura Portugal.
[4] LOARTE A., et al., this conference,
[5] BAZYLEV B. et al. Erosion of macrobrush tungsten armor after multiple intense transient events in ITER, Fusion Eng. Design. 75-79 (2005) 407-411.
[6] BAZYLEV B. et al “Melt damage simulation of W-macrobrush and divertor gaps after multiple transient events in ITER”, 17th PSI Conference, Hefei, China, 2006
[7] GARKUSHA, I., et al., J. Nucl. Mat. **337-339** (2005), 707,
[8] ZHITLUKHIN, A., et al., “Effects of ELMs and disruptions on ITER divertor armour materials” 17th PSI Conference, Hefei, Chaina, 2006
[9] LINKE, J., et al., this conference,
[10] LANDMAN, I., et al., this conference,
[11] GARKUSHA, I., et al., 17th PSI Conference, Hefei, China, 2006
[12] BAZYLEV, B., et al. Energy threshold of brittle destruction for carbon based materials Physica Scripta, **T111**, (2004), 213.
[13] Pestchanyi S. and Linke J. “Simulation of cracks in tungsten under ITER specific heat loads”, 24th Symposium on Fusion Technology, Warsaw, Poland, 2006.